



## Distribution of $^{228}\text{Ra}$ and $^{226}\text{Ra}$ in the Surface Layer of the Black Sea Waters

O. N. Kozlovskaya<sup>1, 2</sup>, D. A. Kremenchutskii<sup>1</sup>, , Iu. G. Shibetskaia<sup>1</sup>,  
V. A. Razina<sup>1</sup>, N. A. Bezhin<sup>1, 2</sup>

<sup>1</sup> Marine Hydrophysical Institute of RAS, Sevastopol, Russian Federation

<sup>2</sup> Sevastopol State University, Sevastopol, Russian Federation

 d.kremenchutskii@mhi-ras.ru

### Abstract

**Purpose.** The purpose of the work is to summarize information on the features of spatial variability of the  $^{226}\text{Ra}$  and  $^{228}\text{Ra}$  concentration fields and the factors influencing these features in the surface water layer of the Black Sea.

**Methods and Results.** The data on spatial variability of the  $^{228}\text{Ra}$  and  $^{226}\text{Ra}$  concentrations in the surface (0.3–3.0 m) layer of the Black Sea obtained during four expeditions were used. The  $^{228}\text{Ra}$  and  $^{226}\text{Ra}$  isotopes were recovered from the seawater samples using the  $\text{MnO}_2$ -based fiber. Their activity was measured by a UMF-2000 alpha-beta radiometer. The data on the content of main elements of the basic biogenic cycle were obtained photometrically.

**Conclusions.** The concentrations of  $^{228}\text{Ra}$  and  $^{226}\text{Ra}$  varied in a range of 17.2 to 172.2 dmp/m<sup>3</sup> and from 38.0 to 270.1 dmp/m<sup>3</sup>, respectively. It is shown that in the region under study, the influence of submarine sources and, presumably, sewage is of a local character and is manifested in an increase of concentrations of these radionuclides or one of them by 1.5–2.3 times. The mesoscale eddies observed in the region of the Southern Coast of Crimea are assumed to affect spatial variability of the radium isotope concentration fields that results in a local decrease or increase in their concentrations by 2.3–2.8 times. It is shown that propagation of the Azov Sea waters in the Black Sea is traced by the  $^{228}\text{Ra}$  and  $^{226}\text{Ra}$  concentration fields: the increased (by 2.3–2.6 times) values of the contents of both isotopes are observed in these areas. It is established that in the areas subjected to the affect of river runoff, the concentration of long-lived radium isotopes is observed to increase with distance from the coast. The spatial scales, on which the influence of a particular source is manifested, are expected to be proportional to its power (flow rate and radionuclides concentration): the higher the power, the greater the distance at which its influence is monitored.

**Keywords:**  $^{228}\text{Ra}$ , radium-228,  $^{226}\text{Ra}$ , radium-226, Black Sea, submarine groundwater discharge, river flow

**Acknowledgements:** The authors are grateful to the captain and crew of the R/V *Professor Vodyanitsky* for their help in carrying out expeditionary operations on the vessel, as well as to the members of the Hydrology and Currents group for providing the data on temperature and salinity. Water samples were taken in the Collective Center R/V *Professor Vodyanitsky* of FSBSI FSC A.O. Kovalevsky Institute of Biology of the Southern Seas. The study was carried out within the framework of a theme of state assignment of Ministry of Science and Higher Education of Russian Federation FNNN-2021-0004.

**For citation:** Kozlovskaya, O.N., Kremenchutskii, D.A., Shibetskaia, Iu.G., Razina, V.A. and Bezhin, N.A., 2023. Distribution of  $^{228}\text{Ra}$  and  $^{226}\text{Ra}$  in the Surface Layer of the Black Sea Waters. *Physical Oceanography*, 30(6), pp. 792-810.

© 2023, O. N. Kozlovskaya, D. A. Kremenchutskii, Iu. G. Shibetskaia, V. A. Razina, N. A. Bezhin

© 2023, Physical Oceanography



## Introduction

Long-lived  $^{226}\text{Ra}$  and  $^{228}\text{Ra}$  are characterized by long half-lives of 1600 and 5.75 years, respectively. These isotopes are continuously produced in the decay series of uranium-238 and thorium-232, which are found mainly in soils, rocks and sediments. Distribution features of radium isotopes in the World Ocean are closely related to their half-life and source of input, as well as to the hydrodynamic conditions observed in a particular area of the ocean [1, 2].

According to the published sources,  $^{226}\text{Ra}$  and  $^{228}\text{Ra}$  are formed directly in the marine environment as a result of the parent nuclear decay (thorium-230 and thorium-232, respectively) and also enter it due to submarine groundwater discharge (SGD) [3–5], river runoff [6, 7], as a result of diffusion from bottom sediments [8] and with precipitation [9]. These isotopes are removed from the marine environment as a result of radioactive decay [10]. Despite the fact that  $^{226}\text{Ra}$  and  $^{228}\text{Ra}$  concentrations in suspended matter are two orders of magnitude lower than in the dissolved form [11–13], the vertical transfer of  $^{226}\text{Ra}$  by settling suspended matter particles (the so-called “biological pump”) is the dominant process of removing this isotope from the upper layers of the World Ocean. This is evidenced by the results of a recently published study [14].

Scientific interest in these radium isotopes is due to the possibility of their use as tracers for studying mixing processes (vertical and horizontal) in coastal [15–17] and deep-sea [2, 18] regions of the World Ocean. They help to find <sup>1</sup>[15] and identify [15, 19–21] fresh water sources in the marine environment and also estimate the volume of fresh water input [4, 22] and the quantity of substances (nutrients, heavy metals, etc.) entering seas and oceans with them [4, 23, 24]. In particular, it was shown in [25–27] that the content of nutrients in SGD areas could be two orders of magnitude higher than background levels.

Great attention is paid to the study of spatial variability of  $^{226}\text{Ra}$  and  $^{228}\text{Ra}$  concentration fields in different areas of the World Ocean [5, 28]. At the same time, detailed studies of the features of such variability of these radionuclides in the Black Sea waters have not previously been carried out.

This paper presents new, as well as previously published [29–31] data on the  $^{226}\text{Ra}$  and  $^{228}\text{Ra}$  content in the surface layer in various Black Sea areas. The present study is aimed to summarize information about spatial variability features of  $^{226}\text{Ra}$  and  $^{228}\text{Ra}$  concentration fields and the factors that determine these features within the economic zone of the Russian Federation in the Black Sea.

## Materials and methods

Sample collection. Expeditionary work was carried out during the 106th (April 18 – May 13, 2019), 116th (April 22 – May 17, 2021) and 121st (April 19 – May 14, 2022) R/V *Professor Vodyanitsky* cruises, as well as during the coastal expedition on July 19, 2020 at Cape Aya. During the expeditions, hydrological measurements and sampling were carried out to determine the concentration of nutrients (silicic acid, dissolved inorganic phosphorus) and the activity of  $^{226}\text{Ra}$  and  $^{228}\text{Ra}$  isotopes.

---

<sup>1</sup> IAEA, 2008. *Nuclear and Isotopic Techniques for the Characterization of Submarine Groundwater Discharge in Coastal Zones. Results of a Coordinated Research Project 2001–2006*. IAEA-TECDOC-1595. Vienna: IAEA, 192 p.

To determine the concentration of nutrients, seawater samples were taken into 125 ml plastic containers, then filtered through membrane filters with a pore diameter of 0.45  $\mu\text{m}$  (Vladisart CJSC, Russia) and frozen for further analysis in a coastal laboratory.

To determine  $^{226}\text{Ra}$  and  $^{228}\text{Ra}$  activity, seawater samples were taken from the 3 m depth (0.3 m during the coastal expedition) into plastic 200–250-liter containers using a UNIPUMP BAVLENETS BV submersible vibration pump 0.12-40-U5 (Sabline Service LLC, Russia), simultaneously filtering through a polypropylene cartridge with a pore diameter of 1  $\mu\text{m}$ . Next, sorption concentration of radium was carried out on board. During the coastal expedition, the collected water samples were transported to the laboratory, where radionuclides were recovered.

$^{226}\text{Ra}$ ,  $^{228}\text{Ra}$  sorption concentration. Recovery of these isotopes was carried out using a two-column method by passing 200–250 L of filtered seawater using a LongerPump WT600-2J peristaltic pump (Longer Precision Pump Co., China) through two columns, each of that was filled with five grams of our own produced  $\text{MnO}_2$ -based fiber. The fiber production technique is thoroughly described in [29];  $^{226}\text{Ra}$ ,  $^{228}\text{Ra}$  sorption efficiency was calculated using the formula also given in this work. According to the results obtained, it averaged  $88 \pm 1\%$  for  $^{226}\text{Ra}$  and  $86 \pm 1\%$  for  $^{228}\text{Ra}$ .

$^{226}\text{Ra}$ ,  $^{228}\text{Ra}$  activity determination. At the end of the expeditionary work, the active component with sorbed radionuclides was washed off the sorbents in a coastal laboratory with a solution containing 2 M HCl and 2 ml of saturated solution of hydroxylamine hydrochloride. Then, radium ions were coprecipitated with barium sulfate. Part of the formed precipitate (100 mg) was transferred to a substrate. The radiochemical preparation procedure is given in detail in [28].

The counting sample prepared in this way was kept for 4–5 days from the separation time of radium isotopes in a Petri dish and measured using UMF-2000 alpha-beta radiometer (Doza LLC RPE, Russia) for at least 8 hours. Three repeated measurements were carried out on 4–5 day, and three more measurements were carried out in 10–12 days after the release of radium isotopes. The error in determining the concentration of radionuclides usually did not exceed 10%.

Determination of nutrient concentration. The main biogenic elements were determined photometrically (RD 52.0.740-2010, RD 52.10.738-2010, RD 52.10.744-2010, RD 52.10.745-2010)<sup>2</sup> [32]: mineral phosphorus from molybdenum blue, silicon from the silicon-molybdenum complex.

A relative error in determining the inorganic phosphorus content was 2.00% for the range of its concentrations of 0–0.21  $\mu\text{M}$  and 1.50% for the range of 2–8  $\mu\text{M}$ . The same for silicic acid: 2.00% for a concentration of 1.1  $\mu\text{M}$ , 0.13% for a concentration of 10.8  $\mu\text{M}$ , 0.50% for a concentration of 18.8  $\mu\text{M}$ .

Hydrological survey. Temperature and salinity measurements during the cruises were carried out using the Ocean Seven 320 plus CTD probe (IDRONAUT S.r.l.,

---

<sup>2</sup> State Fisheries Committee of Russia, 2003. [*Guidelines for the Chemical Analysis of Sea and Fresh Waters during Environmental Monitoring of Fishery Reservoirs and Areas of the World Ocean that Are Promising for Fishing*]. Moscow: VNIRO Publishing, 202 p. Available at: <http://hdl.handle.net/123456789/1554> [Accessed: 18 January 2021] (in Russian).

Italy), during the coastal expedition – with the Condor sounding biophysical complex (*Aquastandard* RPE, TU 431230-006-00241904-2015, code Commodity Nomenclature of Foreign Economic Activity of the EAEU 9027 50 000 0, Declaration of Conformity of the EAEU N RU D-RU.EM03.A.00096/19). Errors in measuring temperature  $\pm 0.05$  °C, salinity  $\pm 0.01$ .

Statistical data analysis was carried out in Statistica® (StatSoft *Inc.*), and maps were generated using Surfer® (Golden Software LLC).

### Concentrations of $^{228}\text{Ra}$ and $^{226}\text{Ra}$ and their ratios in the World Ocean and in the internal basins

Region	Area	<i>S</i>	$^{226}\text{Ra}$ (dpm/m <sup>3</sup> )	$^{228}\text{Ra}$ (dpm/m <sup>3</sup> )	$^{228}\text{Ra}/^{226}\text{Ra}$	Reference
Black Sea	Dniester River	no data	25.2	no data	no data	[34]
	Bug River	no data	234.0	no data	no data	
SE coast of USA	Altamaha River – Noise River	< 1.00	6.0–800.0	12.0–170.0	< 0.19– 2.10	[35]
Arctic Ocean	Alpha-Ridge	no data	104.8	92.0	0.88	[36]
	East Greenland Current	no data	80.0	15.0–38.0	0.19–0.47	[37]
Northern South China Sea	Sanya River Estuary	22.88	154.5	437.5	2.83	[38]
	SSGD*	20.22	2460.0	4350	1.77	
	Sanya Bay	33.77	96.0–119.0	231–380	2.17–3.48	
	Open sea	no data	59.2	117	1.98	
Atlantic Ocean	Amazon River	0.18	41.2	88.8	2.15	[39]
		0.88	37.7	77.0	2.04	
	Amazon River Estuary	35.92–36.26	65.2–75.5	15.9–30.6	0.22–0.40	
		34.01–35.81	69.7–105.7	35.4–262.3	0.51–2.48	
		2.59–34.01	37.7–150.7	70.5–491.8	0.89–3.33	
Croatia	Rivers flowing into the Black and Adriatic seas	< 1.00	392.4–3566.4	154.2–1245.6	0.48–12.00	[40]
Mediterranean Sea	Open sea	no data	75.0	43.0	0.57	[4]
	Alfax Bay (SSGD*)	no data	3300.0	1010.0	0.31	
	Alfax Bay (irrigation canals)	no data	480.0	330.0	0.69	
	Alfax Bay (pore waters)	no data	200.0	1400.0	7.00	
Kara Sea	Ob River	0.01	273.1	409.4	1.44	[41]
		0.03	26.3	41.8	1.39	
	River + sea <sup>⊙</sup>	16.88	46.1	108.6	2.26	
	Open sea	23.81	61.4	138.0	2.15	
	Yenisey River	0.97	32.7	81.3	2.36	
	River + sea <sup>⊙</sup>	9.45	45.8	128.0	2.69	
	Open sea	24.46	56.1	132.0	2.24	
Laptev Sea	Lena River	0.08	85.2	118.8	1.33	
	River + sea <sup>⊙</sup>	0.21	131.1	248.9	1.81	
	Open sea	31.39	72.3	151.6	2.03	
Barents Sea	Open sea	32.80–33.57	63.8–90.5	32.7–56.0	0.49–0.78	

\* SSGD – source of submarine groundwater discharge.

⊙ River and sea water mixing area.

### Results and discussion

$^{228}\text{Ra}$  and  $^{226}\text{Ra}$  distribution in the central Black Sea. Fig. 1 shows spatial distributions of the content of long-lived radium isotopes and their ratios in the surface layer of the Black Sea, obtained by combining the data from three cruises. An increased  $^{228}\text{Ra}$  content is observed in the deep-sea part, and a decreased content is observed in the coastal part. The spatial variability of  $^{226}\text{Ra}$  content is more complex compared to  $^{228}\text{Ra}$ . Thus, the increased and decreased concentration values

are observed both in coastal and deep-sea areas. In the central part,  $^{228}\text{Ra}$  content varies in the range of 47.2–121.7  $\text{dpm}/\text{m}^3$  and averages  $79.3 \pm 27.7 \text{ dpm}/\text{m}^3$ , while  $^{226}\text{Ra}$  content varies in the range of 59.2–86.8  $\text{dpm}/\text{m}^3$  with an average value of  $72.1 \pm 8.9 \text{ dpm}/\text{m}^3$ . The papers [33, 34] present the results of single measurements of  $^{226}\text{Ra}$  in the central part of the sea, according to which its concentration lies in the range of 50.0–102.0  $\text{dpm}/\text{m}^3$ . Therefore, the values obtained in this paper are consistent with the published data on  $^{226}\text{Ra}$  for the central part of the sea. There is no information in the available literature about  $^{228}\text{Ra}$  content in the Black Sea.

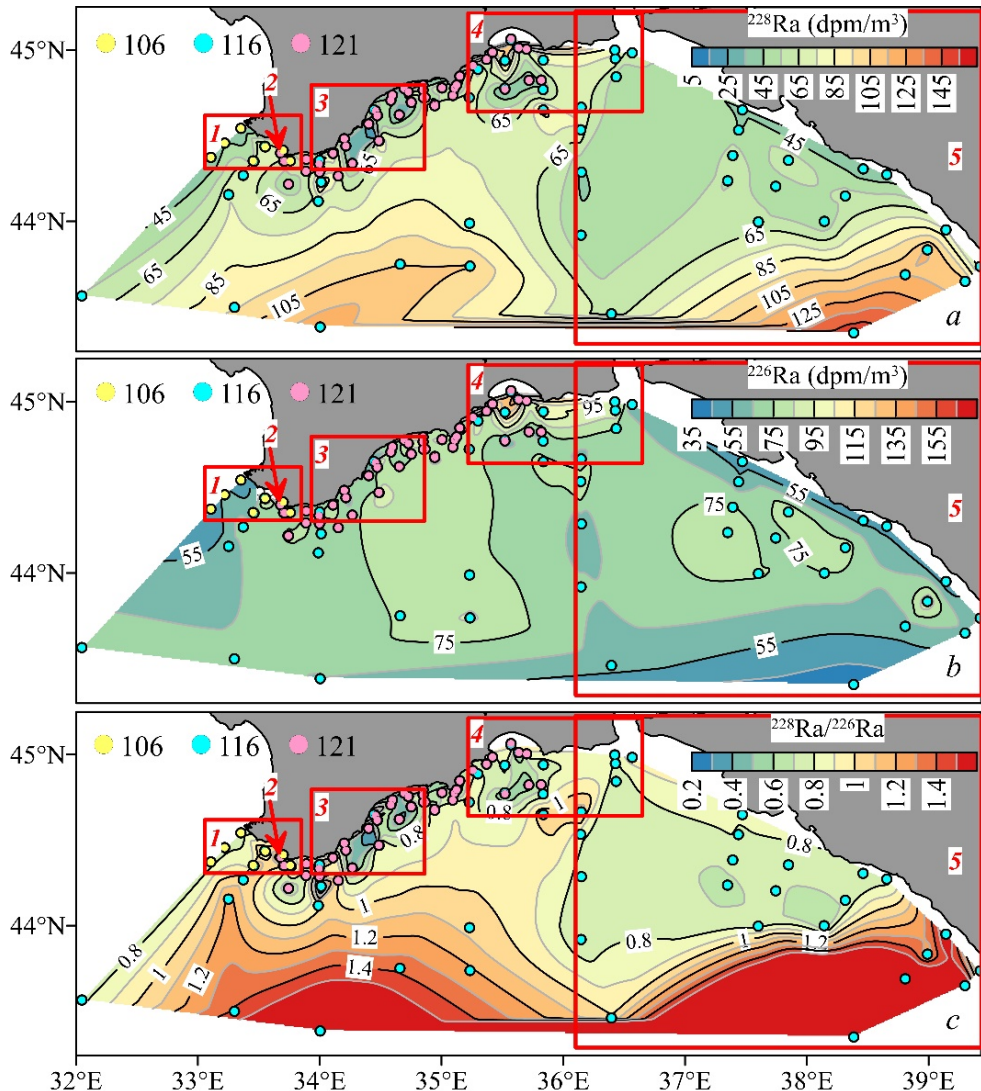


**Fig. 1.** Concentrations of  $^{228}\text{Ra}$  (a) and  $^{226}\text{Ra}$  (b) and their ratio (c) in the Black Sea surface layer (dots show the sampling station locations, their color corresponds to the cruise number of the R/V *Professor Vodyanitsky*; red rectangles indicate the areas under study, red numerals correspond to the ordinal number of these areas)

The spatial variability of  $^{228}\text{Ra}$  to  $^{226}\text{Ra}$  concentration ratio is similar to the spatial variability of  $^{228}\text{Ra}$  concentrations: the increased values are observed in the deep-sea part, and decreased values are observed in the coastal part. In the central part, the ratio is 0.70–1.36 with an average value of 0.97. According to the literature data (table), the ratio of the concentrations of these radionuclides varies in a wide range of 0.17–12.00 in the World Ocean and in the internal basins. This scatter is due to the difference in  $^{228}\text{Ra}$  and  $^{226}\text{Ra}$  content in soils and, as a consequence, in water.

In the considered region, there are various sources of fresh (SGD, river runoff) or desalinated (from the Sea of Azov) waters. To estimate their influence on the spatial variability of  $^{228}\text{Ra}$  and  $^{226}\text{Ra}$  content and their ratio values, this region was divided into 5 areas, shown in Fig. 1.

$^{228}\text{Ra}$  and  $^{226}\text{Ra}$  distribution on the Black Sea shelf in the area of Balaklava (Sevastopol). This area corresponds to area 1 in Fig. 1. The resulting fields of spatial variability of radionuclide concentrations are shown in Fig. 2.

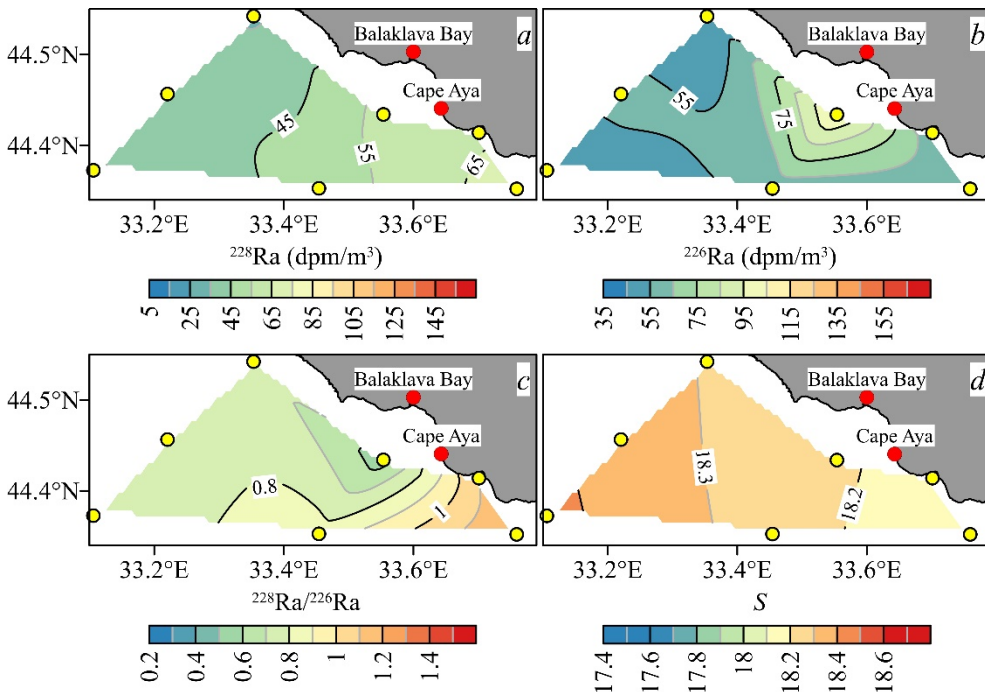


**Fig. 2.** Concentrations of  $^{228}\text{Ra}$  (a) and  $^{226}\text{Ra}$  (b), their ratio (c) and salinity (d) in the Black Sea surface layer based on the data of the 106th cruise of the R/V *Professor Vodyanitsky* (yellow dots show the sampling station locations, red ones – the geographic object positions)

There is a tendency towards a gradual  $^{228}\text{Ra}$  content decrease from the southwest ( $70.9 \text{ dpm/m}^3$ ) to the northeast ( $33.5 \text{ dpm/m}^3$ ) of the considered area (Fig. 2, a). It is noteworthy that the opposite trend is observed in the salinity field (Fig. 2, d). The correlation analysis results indicate the presence of a strong

relationship between these parameters ( $r = -0.90$ ,  $p < 0.01$ ). At the station closest to the exit from Balaklava Bay (Fig. 2, *b*), a maximum concentration of  $^{226}\text{Ra}$  ( $106.6 \text{ dmp/m}^3$ ) is observed, which is 2.4 times higher than this radionuclide concentration at the “background” station ( $44.8 \text{ dmp/m}^3$ ). The station farthest from the coast was taken as the “background” one. In this case, it is the leftmost station in Fig. 2, *b*. According to the literature data, there is a release of sewage water into the open sea exceeding  $3 \text{ mln m}^3/\text{year}$  at the exit from Balaklava Bay [42], as well as a source of SGD<sup>3</sup>. It is possible that these sources are responsible for the increased  $^{226}\text{Ra}$  content. To confirm or refute this assumption, it is necessary to obtain the data on the content of radium isotopes in these sources. Note that the influence of the proposed sources is not observed in  $^{228}\text{Ra}$  concentration field. The ratio of radionuclide concentrations (Fig. 2, *c*) was minimal at the point with the maximum  $^{226}\text{Ra}$  concentration (0.55, Fig. 2, *b*) and maximum in the eastern part of the region (1.21). Correlation analysis results indicate that there is no relationship between the spatial variability of  $^{228}\text{Ra}$  and  $^{226}\text{Ra}$  concentrations ( $r = 0.45$ ,  $p = 0.31$ ).

$^{228}\text{Ra}$  and  $^{226}\text{Ra}$  distribution near Cape Aya. The cape is located in area 1, its position is marked by an arrow in Fig. 1 and a marker in Fig. 2. This area (Fig. 3) is of interest because, according to the published data [43, 44], there is a large submarine spring with a flow rate of  $4100\text{--}13900 \text{ m}^3/\text{day}$  in the Ekaterininsky Grotto (a karst cavity open to the sea on one side, under a rocky cliff near Cape Aya).

Increased  $^{228}\text{Ra}$  and  $^{226}\text{Ra}$  concentrations were recorded in the grotto and varied in the ranges of  $102.7\text{--}135.9 \text{ dmp/m}^3$  (average  $118.9 \text{ dmp/m}^3$ ) and  $227.7\text{--}270.1 \text{ dmp/m}^3$  (average  $247.9 \text{ dmp/m}^3$ ) respectively (Fig. 3, *a, b*). In addition to high concentrations of radionuclides in the grotto, minimum values of salinity and temperature ( $13.04$  and  $21.39 \text{ }^\circ\text{C}$ , respectively) and maximum values of nutrient concentration ( $37.80$  and  $0.23 \text{ }\mu\text{M}$  for silicic acid and dissolved inorganic phosphorus, respectively) are also observed (Fig. 3, *d–g*). The data on the vertical distribution of salinity (not shown in the figure) indicate that lighter desalinated waters are distributed in a narrow layer  $\sim 0.5 \text{ m}$  thick. The data on spatial variability in the concentration of nutrients and salinity indicate the presence of two groundwater outflow points in the grotto, which is consistent with the results of [30, 45, 46].

At a distance of  $\sim 100 \text{ m}$  from the grotto,  $^{228}\text{Ra}$  concentration decreased by 1.6–2.2 times up to  $53.5 \text{ dmp/m}^3$ ,  $^{226}\text{Ra}$  concentration decreased by 1.6–2.3 times to  $107.3 \text{ dmp/m}^3$ , the silicic acid and dissolved inorganic phosphorus concentration – by 5.4–36.9 times up to  $0.80 \text{ }\mu\text{M}$  and by 1.5–16 times up to  $< 0.01 \text{ }\mu\text{M}$ , respectively; the temperature and salinity increased by 1.7 times up to  $24.76 \text{ }^\circ\text{C}$  and by 1.2 times up to 18.13, respectively. Correlation analysis results show a strong relationship between the variability of  $^{228}\text{Ra}$  and  $^{226}\text{Ra}$  concentrations ( $r = 0.85$ ,  $p = 0.03$ ), as well

---

<sup>3</sup> Kondratev, S., 2020. [Submarine Waters of Crimea]. *Kommersant. Nauka*, (33), p. 28. Available at: <https://www.kommersant.ru/doc/4566221> [Accessed: 20 May 2023] (in Russian).



as between  $^{228}\text{Ra}$ ,  $^{226}\text{Ra}$  variability and salinity concentrations with correlation coefficients of  $-0.89$  ( $p = 0.01$ ) and  $-0.93$  ( $p < 0.01$ ). Thus, there is a concentration decrease of both isotopes as fresh water becomes diluted with seawater.

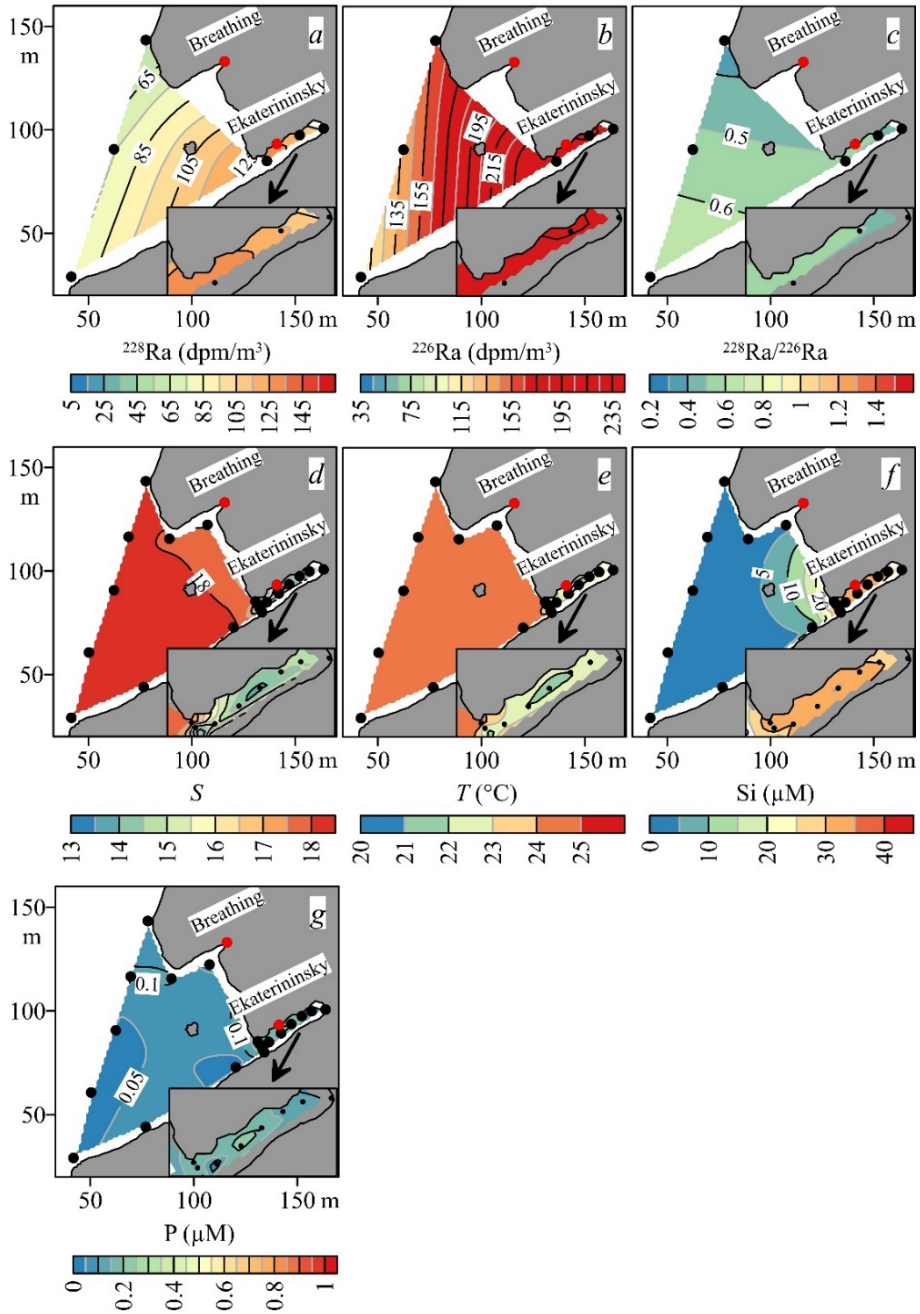


**Fig. 3.** Concentrations of  $^{228}\text{Ra}$  (a) and  $^{226}\text{Ra}$  (b), their ratio (c), salinity (d) and temperature (e), concentrations of silicic acid (f) and dissolved inorganic phosphorus (g) in the karst cavity and the adjacent areas (black dots show the sampling station locations, red ones – the names of grottoes)



The maximum value of  $^{228}\text{Ra} / ^{226}\text{Ra}$  concentration ratio was observed in the southwestern part of the polygon (0.71), the minimum – at its northern point (0.34). The average concentration ratio in the grotto was  $0.48 \pm 0.05$ . The observed minimum value of radionuclide concentration ratio in the northern part may be due to the mixing of the Ekaterininsky Grotto waters with the Breathing Grotto waters, located to the north (Fig. 3), since during low winds the distribution of waters from “the Ekaterininsky Grotto in the northern direction dominates”<sup>4</sup>. This assumption is also supported by the data on spatial salinity variability – the “plume” of lowered salinity values to the north of Ekaterininsky Grotto (Fig. 3, *d*). The correlation analysis results indicate that there is no relationship between the spatial variability of the concentration and the salinity ratio ( $r = 0.21$ ,  $p = 0.68$ ).

$^{228}\text{Ra}$  and  $^{226}\text{Ra}$  distribution in the Southern Coast of Crimea region. This area corresponds to area 3 in Fig. 1. According to the 121st cruise data, an area of low  $^{228}\text{Ra}$  and high  $^{226}\text{Ra}$  contents was observed here; the radionuclide concentrations were 17.2–24.1 and 73.2–135.7 dpm/m<sup>3</sup>, respectively (Fig. 4, *a, b*). At the periphery of this area,  $^{228}\text{Ra}$  concentration increased to 67.5 dpm/m<sup>3</sup>, and  $^{226}\text{Ra}$  concentration decreased to 57.4 dpm/m<sup>3</sup>. The correlation analysis results indicate that there is no relationship between the spatial variability of these radionuclides ( $r = -0.46$ ,  $p = 0.11$ ). The minimum  $^{228}\text{Ra}/^{226}\text{Ra}$  ratio (0.13) was observed at the station closest to Alushta (Fig. 4, *c*). In the southern part of the region under study it increased to 1.06. Without presenting a map, it's noted that in the considered area the spatial variability of salinity was insignificant (on average 18.55) with a standard deviation of 0.03. For this reason, there was no statistically significant correlation between  $^{228}\text{Ra}$ ,  $^{226}\text{Ra}$  concentrations and their relationship with salinity, which was statistically significant at the 95% significance level.

In our opinion, such spatial variability in  $^{228}\text{Ra}$ ,  $^{226}\text{Ra}$  concentrations can be explained by one of the two factors: upwelling of deep waters by a cyclone or the combined influence of a cyclone and submarine sources.

According to the data from [47], cyclonic and anticyclonic eddies can be observed in this area. An indirect argument proving that such structures were actually observed is evidenced, for example, by the data on depths of the cold intermediate layer (CIL) core and the isopycnal 14.4 rel. units on the 121st cruise of R/V *Professor Vodyanitsky*. The analyzed isopycnal was selected based on its maximum value observed at the shallowest station. Fig. 4, *d, e* shows that the depth varies in the ranges of 38–103 and 26–58 m for the CIL position and isopycnal 14.4 rel. units respectively. In the studied area, minimum depths are observed. Since there was a decrease in  $^{228}\text{Ra}$  content and an increase in  $^{226}\text{Ra}$  concentration, it can be assumed that this is a manifestation of the cyclone, which is located in the studied area and elevates water from deeper layers to the surface. In general, with increasing depth,  $^{228}\text{Ra}$  concentration decreases and  $^{226}\text{Ra}$  concentration increases due to the difference in half-lives [1]. There are no data on the vertical distribution of concentrations of these radionuclides that could confirm or refute the above or the following hypothesis.

---

<sup>4</sup> Ivanov, V.A., 2013. [Submarine Groundwater Discharge in the Area of Cape Aya. Research Methodology. Features of Surface Flow and Manifestation of Submarine Waters in the Field of Hydrological and Optical Characteristics (According to Experimental Studies 2013): Research Report]. Sevastopol: MHI of NASU Publishing, 320 p. (in Russian).

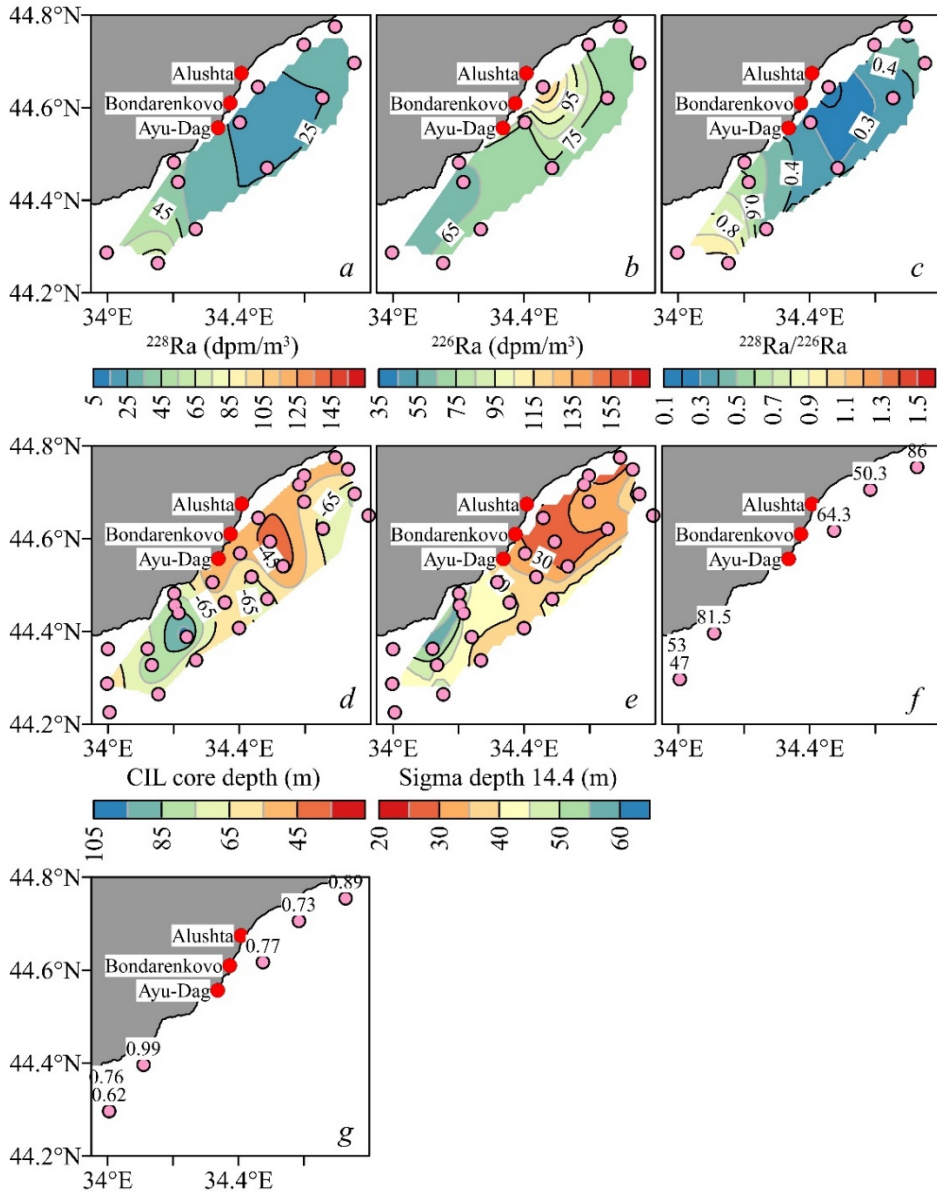


**Fig. 4** Concentrations of  $^{228}\text{Ra}$  (a) and  $^{226}\text{Ra}$  (b), their ratio (c), depths of CIL (d) and sigma 14.4 (e) during the first passage of the grid of stations, and  $^{228}\text{Ra}$  concentration (f) and  $^{228}\text{Ra} / ^{226}\text{Ra}$  ratio (g) at the re-passage of the stations in the 121st cruise of the R/V *Professor Vodyanitsky* (pink dots show the station locations, red ones – the geographical object positions)

The second hypothesis considers the submarine water transfer by a passing cyclone in the study area. Thus, according to the data from [48, 49], the action of two submarine sources of fissure-vein origin is assumed in the Southern Coast of Crimea: in the southern part of the Ayu-Dag Mountain and near the village of Bondarenkovo. The work [48] reports that submarine discharge of under-channel runoff is located at a distance from the coast near Alushta. Eastward there is an area discharge of fissure-karst waters [48]. There are no data on the content of radium

isotopes and their ratios in these sources. Without citing maps, it's noted that the spatial variability of salinity and temperature in the area of lowered  $^{228}\text{Ra}$  concentrations compared to neighboring stations does not make it possible to confirm a submarine source presence at these stations.

Ten days later, two seawater samples with a low  $^{228}\text{Ra}$  content were taken in the area under consideration on the way back to Sevastopol (Fig. 4, *f*, *g*). The radionuclide content in them was 64.3 and 50.3 dpm/m<sup>3</sup>, which corresponds to the activity values previously observed in the southwestern part of this area. The  $^{228}\text{Ra}/^{226}\text{Ra}$  activity ratio at these two stations increased to 0.77, which is also close to the values previously observed in the southwestern part of the polygon. In general, when compared with  $^{228}\text{Ra}$  concentration values and  $^{228}\text{Ra}/^{226}\text{Ra}$  ratio at the nearest northeastern and southwestern stations, they remain relatively low.

$^{226}\text{Ra}$  and  $^{228}\text{Ra}$  distribution in the Black Sea in the eastern Crimea. The Azov Sea is characterized by a salinity lower by 6.50–7.50 compared to the Black Sea [50]. Penetrating through the Kerch Strait, the waters can spread in western and eastern directions depending on wind conditions [50]. In a western direction, they are transported along the coast in a relatively narrow stream 1–10 km wide and reach Cape Chauda or Cape Meganom, where they are separated from the shore. Further, the jet width can increase to 30 km or break up into separate spots. In some cases, distribution of the Azov Sea waters can be traced to Cape Khersones (Sevastopol).

Most of the seawater samples in the Cape Chauda–Kerch Strait area were taken during the 116th R/V *Professor Vodyanitsky* cruise (Fig. 5). At the two stations closest to the Kerch Strait, elevated concentrations of  $^{228}\text{Ra}$  (57.7–78.2 dpm/m<sup>3</sup>) and  $^{226}\text{Ra}$  (60.2–93.1 dpm/m<sup>3</sup>) are observed. At a station located seawards,  $^{228}\text{Ra}$  and  $^{226}\text{Ra}$  concentrations decrease to 50.3 and 73.6 dpm/m<sup>3</sup>, respectively. A series of elevated concentrations of these radionuclides can be monitored from the strait towards the Feodosiya Gulf. Most likely, its appearance is due precisely to the spread of the Azov Sea waters. This is also supported by the data on the spatial variability of salinity (Fig. 5, *d*) and the ratio of these radionuclide concentrations (Fig. 5, *c*).

As noted above, the Azov Sea waters, which are characterized by low salinity and high content of both isotopes, can enter the Feodosiya Gulf. At stations located in the bay itself and near it,  $^{228}\text{Ra}$  and  $^{226}\text{Ra}$  concentrations reach 172.3 and 169.8 dpm/m<sup>3</sup>, respectively (Fig. 5, *a*), which is 2.2–2.8 times higher than near the Kerch Strait. Taking into account the spatial distribution of absolute salinity values and the ratios of radium concentrations (17.40–18.20 and 0.67–1.01), it can be assumed that the source of increased  $^{228}\text{Ra}$  and  $^{226}\text{Ra}$  concentrations in the gulf is the Azov Sea waters. Otherwise, a change in the concentration ratio of these radionuclides would be expected. Most likely, the lower values of radionuclide concentrations at the stations closest to the Kerch Strait are due to the fact that these stations are located 8–14 km from the coast, which is quite far considering the width of the Azov Sea water stream (1–10 km). Most likely, these stations were located on the jet periphery. It is worth noting that the results of the study of spatial temperature and salinity variability, presented in the available literature<sup>3</sup>, indicate the presence of a submarine source located at the gulf bottom (~ 30 m). At the same time, due to work restrictions in the bay, the authors of this study were unable to identify the exact location of this source. We shall note that our analysis of the data on vertical distribution of temperature and salinity (not shown in Fig. 5) did not make it possible to confirm the existence of such a source.

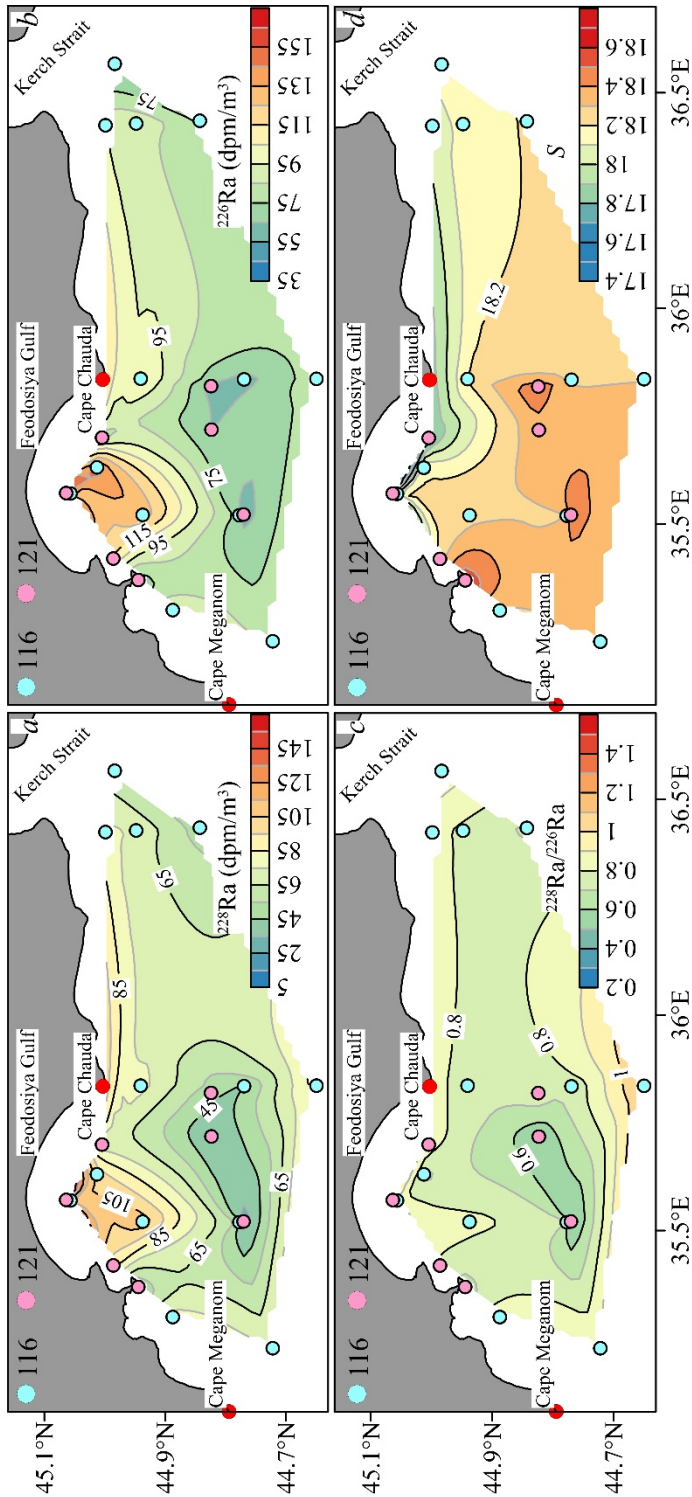


**Fig. 5.** Concentrations of  $^{228}\text{Ra}$  (a) and  $^{226}\text{Ra}$  (b), their ratio (c) and salinity (d) (pink and cyan dots show the station locations in two cruises, red ones – the geographical object positions)

$^{226}\text{Ra}$  and  $^{228}\text{Ra}$  distribution of in the eastern Black Sea. This area corresponds to area 5 in Fig. 1. Its difference from those considered above is the presence of rivers flowing into the sea. The data on the spatial variability of  $^{228}\text{Ra}$  and  $^{226}\text{Ra}$  concentration fields are shown in Fig. 6.

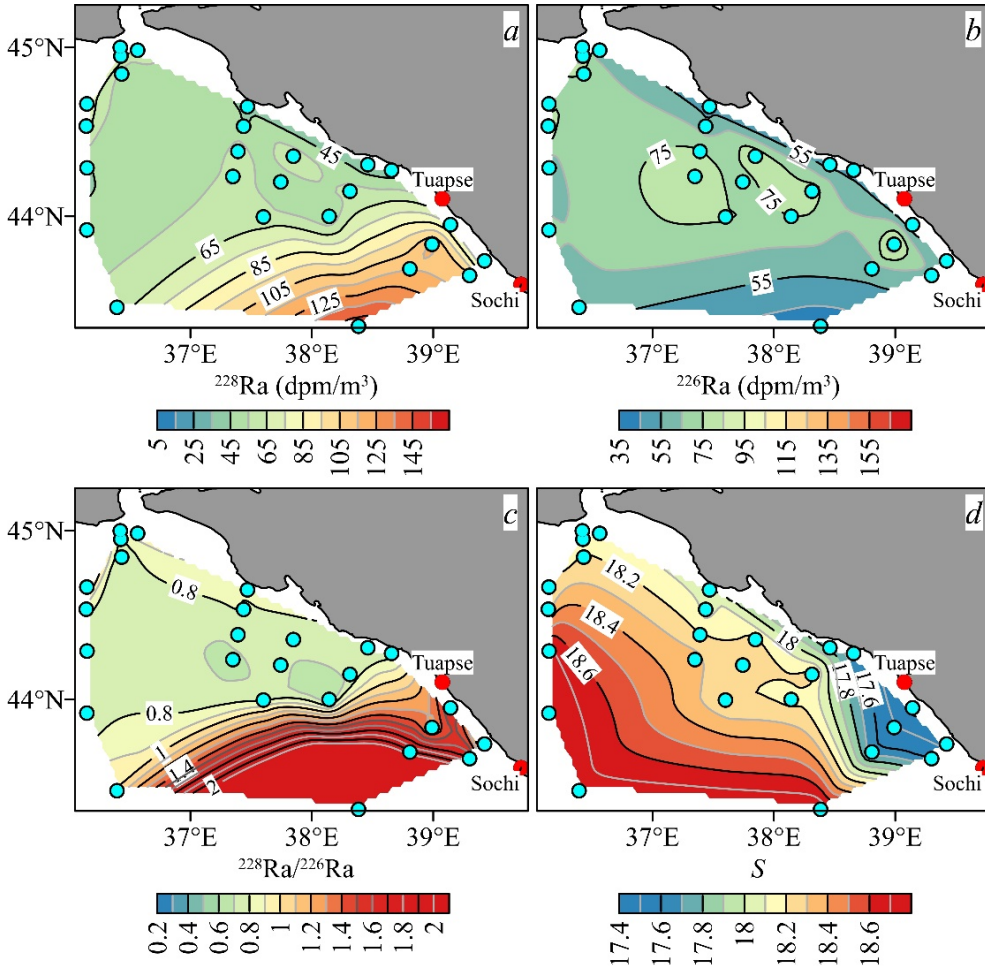


**Fig. 6** Concentrations of  $^{228}\text{Ra}$  (a) and  $^{226}\text{Ra}$  (b), their ratio (c) and salinity (d) (cyan dots show the station locations in the 116th cruise of the R/V *Professor Vodyanitsky*, red ones – the geographical object positions)

$^{228}\text{Ra}$  and  $^{226}\text{Ra}$  content varied spatially in the ranges of 37.9–153.0 and 37.9–95.5  $\text{dpm}/\text{m}^3$ , respectively (Fig. 6, a, b), the value of their concentration ratio was in the range of 0.59–4.03 (Fig. 6, c). It is noteworthy that, despite the differences in the initial content of radionuclides near the eastern coast of the Black Sea, in all cases there was an increase in their concentration along the transect from the coastal station to the next one. Increased concentrations of  $^{228}\text{Ra}$  and high values of  $^{228}\text{Ra}/^{226}\text{Ra}$  ratio are observed in the eastern part of the region under consideration between Sochi and Tuapse. Most likely, this is due to the influence of river runoff.

Thus, at the station closest to the shore, located at a distance of  $\sim 10$  km from it, salinity was 17.40 (Fig. 6, *d*),  $^{228}\text{Ra}$  concentration was  $75.8 \text{ dpm/m}^3$  and the concentration ratio was 1.62. As we moved away from the coast, salinity increased to 18.80,  $^{228}\text{Ra}$  concentration to  $153.0 \text{ dpm/m}^3$  and concentration ratio to 4.03. Most likely, such spatial variability of isotope concentrations is associated with desorption of radionuclides from suspended matter entering the marine environment with river waters. Therefore, the activity of radium adsorbed on riverine suspended matter can be several times greater than in a dissolved form in river water [51]. When river water is mixed with sea water, on the one hand, the process of suspended matter coagulation is intensified with its subsequent sedimentation into bottom sediments and, on the other hand, desorption of radium isotopes from it starts. Similar results were obtained in [19, 52], which analyzed the variability of  $^{228}\text{Ra}$  and  $^{226}\text{Ra}$  contents as riverine water undergoes changes with the distance from the estuary. The concentration ratio increase observed in this study may be due to the difference in the content of radium isotopes on the suspended matter, as well as the rate of desorption of these radionuclides from the suspended matter (since their sorption rate is also different [23, 31]).

### Conclusions

This paper presents *in situ* data on the spatial variability of  $^{228}\text{Ra}$  and  $^{226}\text{Ra}$  concentrations and their ratio in the surface layer of the Black Sea. Thus, the content of radionuclides varied spatially in a wide range of  $17.2\text{--}172.2 \text{ dmp/m}^3$  for  $^{228}\text{Ra}$  and  $38.0\text{--}270.1 \text{ dmp/m}^3$  for  $^{226}\text{Ra}$ . The activity ratio of  $^{228}\text{Ra}$  to  $^{226}\text{Ra}$  was  $0.13\text{--}4.03$ . The spatial variability of  $^{228}\text{Ra}$  concentration shows a tendency to decrease from the deep sea to the shelf.  $^{226}\text{Ra}$  concentration field, on the one hand, is more uniform compared to  $^{228}\text{Ra}$  and as a result the spatial variability of  $^{228}\text{Ra}/^{226}\text{Ra}$  ratio is generally similar to the spatial variability of  $^{228}\text{Ra}$  concentration. On the other hand, the concentration field has a more complex character: relatively increased and decreased  $^{226}\text{Ra}$  concentrations were observed both in the coastal and deep-sea parts.

Influence of fresh (SGD, river runoff) or desalinated (Azov Sea input) water sources on  $^{228}\text{Ra}$  and  $^{226}\text{Ra}$  distribution was analyzed. It is shown that in the study area the influence of submarine sources and, presumably, sewage drains is local in nature and is showed in an increase in the concentration of these radionuclides or one of them by  $1.5\text{--}2.3$  times. It has been suggested that mesoscale eddies in the area of the Southern Coast of Crimea can influence the spatial variability of radium isotope concentration fields leading to a local decrease or increase in their concentration by  $2.3\text{--}2.8$  times. It is shown that the distribution of the Azov Sea waters in the Black Sea is traced by an increase in  $^{228}\text{Ra}$  and  $^{226}\text{Ra}$  concentrations. In particular, according to the data on  $^{228}\text{Ra}/^{226}\text{Ra}$  ratio, it was found out that concentration values of these radionuclides that elevated by  $2.3\text{--}2.6$  times in the Feodosiya Gulf are due to the spread of the Azov Sea waters. It has been shown that in areas exposed to the river runoff influence, there is an increase in the concentration of long-lived radium isotopes with the distance from the coast. This increase is likely due to desorption of radionuclides from the particles of

suspended matter entering with river water. It should be expected that the spatial scales on which a particular source influence is manifested are proportional to their power (flow rate and concentration of radionuclides): the higher the power, the greater the distance of the observed source influence. Thus, for example, SGD influence at Cape Aya was monitored by  $^{228}\text{Ra}$  approximately a hundred meters from the source, while the influence of the Azov Sea waters was monitored 80 km from the Kerch Strait.

#### REFERENCES

1. Rutgers van der Loeff, M.M. and Geibert, W., 2008. Chapter 7 U- and Th-Series Nuclides as Tracers of Particle Dynamics, Scavenging and Biogeochemical Cycles in the Oceans. In: S. Krishnaswami and J. K. Cochran, eds., 2008. *U-Th-Series Nuclides in Aquatic Systems*. Radioactivity in the Environment, vol. 13. Amsterdam: Elsevier, pp. 227-268. doi:10.1016/S1569-4860(07)00007-1
2. Broecker, W.S., Goddard, J. and Sarmiento, J.L., 1976. The Distribution of  $^{226}\text{Ra}$  in the Atlantic Ocean. *Earth and Planetary Science Letters*, 32(2), pp. 220-235. doi:10.1016/0012-821X(76)90063-7
3. Gonnee, M.E., Charette, M.A., Liu, Q., Herrera-Silveira, J.A. and Morales-Ojeda, S.M., 2014. Trace Element Geochemistry of Groundwater in a Karst Subterranean Estuary (Yucatan Peninsula, Mexico). *Geochimica et Cosmochimica Acta*, 132, pp. 31-49. doi:10.1016/j.gca.2014.01.037
4. Rodellas, V., Garcia-Orellana, J., Trezzi, G., Masqué, P., Stieglitz, T.C., Bokuniewicz, H., Cochran, J.K. and Berdalet, E., 2017. Using the Radium Quartet to Quantify Submarine Groundwater Discharge and Porewater Exchange. *Geochimica et Cosmochimica Acta*, 196, pp. 58-73. doi:10.1016/j.gca.2016.09.016
5. Moore, W.S., Sarmiento, J.L. and Key, R.M., 2008. Submarine Groundwater Discharge Revealed by  $^{228}\text{Ra}$  Distribution in the Upper Atlantic Ocean. *Nature Geoscience*, 1(5), pp. 309-311. doi:10.1038/ngeo183
6. Su, N., Du, J., Duan, Z., Deng, B. and Zhang, J., 2015. Radium Isotopes and Their Environmental Implications in the Changjiang River System. *Estuarine, Coastal and Shelf Science*, 156, pp. 155-164. doi:10.1016/j.ecss.2014.12.017
7. Carroll, J., Falkner, K.K., Brown, E.T. and Moore, W.S., 1993. The Role of the Ganges-Brahmaputra Mixing Zone in Supplying Barium and  $^{226}\text{Ra}$  to the Bay of Bengal. *Geochimica et Cosmochimica Acta*, 57(13), pp. 2981-2990. doi:10.1016/0016-7037(93)90287-7
8. Beck, A.J., Rapaglia, J.P., Cochran, J.K., Bokuniewicz, H.J. and Yang, S., 2008. Submarine Groundwater Discharge to Great South Bay, NY, Estimated Using Ra Isotopes. *Marine Chemistry*, 109(3-4), pp. 279-291. doi:10.1016/j.marchem.2007.07.011
9. Charette, M.A., Moore, W.S. and Burnett, W.C., 2008. Chapter 5 Uranium- and Thorium-Series Nuclides as Tracers of Submarine Groundwater Discharge. In: S. Krishnaswami, J. K. Cochran, eds., 2008. *U-Th-Series Nuclides in Aquatic Systems*. Radioactivity in the Environment, vol. 13. Amsterdam: Elsevier, pp. 155-191. doi:10.1016/s1569-4860(07)00005-8
10. Garcia-Orellana, J., Rodellas, V., Tamborski, J., Diego-Feliu, M., van Beek, P., Weinstein, Y., Charette, M., Alorda-Kleinglass, A., Michael, H.A. [et al.], 2021. Radium Isotopes as Submarine Groundwater Discharge (SGD) Tracers: Review and Recommendations. *Earth-Science Reviews*, 220, 103681. doi:10.1016/j.earscirev.2021.103681



11. Van Beek, P., François, R., Conte, M., Reyss, J.-L., Souhaut, M. and Charette, M., 2007.  $^{228}\text{Ra}/^{226}\text{Ra}$  and  $^{226}\text{Ra}/\text{Ba}$  Ratios to Track Barite Formation and Transport in the Water Column. *Geochimica et Cosmochimica Acta*, 71(1), pp. 71-86. doi:10.1016/j.gca.2006.07.041
12. Van Beek, P., Sternberg, E., Reyss, J.-L., Souhaut, M., Robin, E. and Jeandel, C., 2009.  $^{228}\text{Ra}/^{226}\text{Ra}$  and  $^{226}\text{Ra}/\text{Ba}$  Ratios in the Western Mediterranean Sea: Barite Formation and Transport in the Water Column. *Geochimica et Cosmochimica Acta*, 73(16), pp. 4720-4737. doi:10.1016/j.gca.2009.05.063
13. Van Beek, P., François, R., Honda, M., Charette, M.A., Reyss, J.-L., Ganeshram, R., Monnin, C. and Honjo, S., 2022. Fractionation of  $^{226}\text{Ra}$  and Ba in the Upper North Pacific Ocean. *Frontiers in Marine Science*, 9, 859117. doi:10.3389/fmars.2022.859117
14. Xu, B., Cardenas, M.B., Santos, I.R., Burnett, W.C., Charette, M.A., Rodellas, V., Li S., Lian, E. and Yu, Z., 2022. Closing the Global Marine  $^{226}\text{Ra}$  Budget Reveals the Biological Pump as a Dominant Removal Flux in the Upper Ocean. *Geophysical Research Letters*, 49(12), e2022GL098087. doi:10.1029/2022GL098087
15. Moore, W.S., 2000. Determining Coastal Mixing Rates Using Radium Isotopes. *Continental Shelf Research*, 20(15), pp. 1993-2007. doi:10.1016/S0278-4343(00)00054-6
16. Iyengar, M.A.R., Kannan, V. and Rao, K.N., 1989.  $^{228}\text{Ra}/^{226}\text{Ra}$  Ratios in Coastal Waters of Kalpakkam. *Journal of Environmental Radioactivity*, 9(2), pp. 163-180. doi:10.1016/0265-931X(89)90022-2
17. Hsieh, Y.-T., Geibert, W., van Beek, P., Stahl, H., Aleynik, D. and Henderson, G.M., 2013. Using the Radium Quartet ( $^{228}\text{Ra}$ ,  $^{226}\text{Ra}$ ,  $^{224}\text{Ra}$ , and  $^{223}\text{Ra}$ ) to Estimate Water Mixing and Radium Inputs in Loch Etive, Scotland. *Limnology and Oceanography*, 58(3), pp. 1089-1102. doi:10.4319/lo.2013.58.3.1089
18. Ku, T.-L., Luo, S., Kusakabe, M. and Bishop, J.K.B., 1995.  $^{228}\text{Ra}$ -Derived Nutrient Budgets in the Upper Equatorial Pacific and the Role of "New" Silicate in Limiting Productivity. *Deep Sea Research Part II: Topical Studies in Oceanography*, 42(2-3), pp. 479-497. doi:10.1016/0967-0645(95)00020-Q
19. Plater, A.J., Ivanovich, M. and Dugdale, R.E., 1995.  $^{226}\text{Ra}$  Contents and  $^{228}\text{Ra}/^{226}\text{Ra}$  Activity Ratios of the Fenland Rivers and The Wash, Eastern England: Spatial and Seasonal Trends. *Chemical Geology*, 119(1-4), pp. 275-292. doi:10.1016/0009-2541(94)00109-1
20. Moore, W.S., 2006. Radium Isotopes as Tracers of Submarine Groundwater Discharge in Sicily. *Continental Shelf Research*, 26(7), pp. 852-861. doi:10.1016/j.csr.2005.12.004
21. Moore, W.S., 2003. Sources and Fluxes of Submarine Groundwater Discharge Delineated by Radium Isotopes. *Biogeochemistry*, 66(1-2), pp. 75-93. doi:10.1023/B:BIOG.0000006065.77764.a0
22. Burnett, W.C., Aggarwal, P.K., Aureli, A., Bokuniewicz, H., Cable, J.E., Charette, M.A., Kontar, E., Krupa, S., Kulkarni, K.M. [et al.], 2006. Quantifying Submarine Groundwater Discharge in the Coastal Zone via Multiple Methods. *Science of the Total Environment*, 367(2-3), pp. 498-543. doi:10.1016/j.scitotenv.2006.05.009
23. Gao, J.-Y., Wang, X.-J., Zhang, Y. and Li, H.-L., 2018. Estimating Submarine Groundwater Discharge and Associated Nutrient Inputs into Daya Bay during Spring Using Radium Isotopes. *Water Science and Engineering*, 11(2), pp. 120-130. doi:10.1016/j.wse.2018.06.002
24. Liu, J., Liu, D. and Du, J., 2022. Radium-Traced Nutrient Outwelling from the Subei Shoal to the Yellow Sea: Fluxes and Environmental Implication. *Acta Oceanologica Sinica*, 41(6), pp. 12-21. doi:10.1007/s13131-021-1930-z
25. Tamborski, J., van Beek, P., Conan, P., Pujo-Pay, M., Odobel, C., Ghiglione, J.-F., Seidel, J.-L., Arfib, B., Diego-Feliu, M. [et al.], 2020. Submarine Karstic Springs as a Source of Nutrients and

- Bioactive Trace Metals for the Oligotrophic Northwest Mediterranean Sea. *Science of The Total Environment*, 732, 139106. doi:10.1016/j.scitotenv.2020.139106
26. Niencheski, L.F.H., Windom, H.L., Moore, W.S. and Jahnke, R.A., 2007. Submarine Groundwater Discharge of Nutrients to the Ocean along a Coastal Lagoon Barrier, Southern Brazil. *Marine Chemistry*, 106(3-4), pp. 546–561. doi:10.1016/j.marchem.2007.06.004
  27. Rahman, S., Tamborski, J.J., Charette, M.A. and Cochran K.J., 2019. Dissolved Silica in the Subterranean Estuary and the Impact of Submarine Groundwater Discharge on the Global Marine Silica Budget. *Marine Chemistry*, 208, pp. 29-42. doi:10.1016/j.marchem.2018.11.006
  28. Xing, N., Chen, M., Huang, Y., Cai, P. and Qiu, Y., 2003. Distribution of <sup>226</sup>Ra in the Arctic Ocean and the Bering Sea and Its Hydrologic Implications. *Science in China Series D: Earth Sciences*, 46(5), pp. 516-528. doi:10.1360/03yd9045
  29. Dovhyi, I.I., Kremenchutskii, D.A., Bezhin, N.A., Shibetskaya, Yu.G., Tovarchii, Ya.Yu., Egorin, A.M., Tokar, E.A. and Tananaev, I.G., 2020. MnO<sub>2</sub> Fiber as a Sorbent for Radionuclides in Oceanographic Investigations. *Journal of Radioanalytical and Nuclear Chemistry*, 323(1), pp. 539-547. doi:10.1007/s10967-019-06940-9
  30. Dovhyi, I.I., Bezhin, N.A., Kremenchutskii, D.A., Kozlovskaya, O.N., Chepyzhenko, A.I., Verterich, A.V., Tovarchii, Ya.Yu., Shibetskaya, Yu.G. and Chaikin, D.Yu., 2021. Studying Submarine Groundwater Discharge at the Cape Ayia: A Multi-Tracer Approach. *Physical Oceanography*, 28(1), pp. 52-66. doi:10.22449/1573-160X-2021-1-52-66
  31. Kozlovskaya, O.N., Shibetskaia, I.G., Bezhin, N.A. and Tananaev, I.G., 2023. Estimation of <sup>226</sup>Ra and <sup>228</sup>Ra Content Using Various Types of Sorbents and Their Distribution in the Surface Layer of the Black Sea. *Materials*, 16(5), 1935. doi:10.3390/ma16051935
  32. Wurl, O., ed., 2009. *Practical Guidelines for the Analysis of Seawater*. Boca Raton: CRC Press, 408 p. doi:10.1201/9781420073072
  33. Falkner, K.K., O'Neill, D.J., Todd, J.F., Moore, W.S. and Edmond, J.M., 1991. Depletion of Barium and Radium-226 in Black Sea Surface Waters over the Past Thirty Years. *Nature*, 350, pp. 491-494. doi:10.1038/350491a0
  34. Moore, W.S. and Falkner, K.K., 1999. Cycling of Radium and Barium in the Black Sea. *Journal of Environmental Radioactivity*, 43(2), pp. 247-254. doi:10.1016/s0265-931x(98)00095-2
  35. Moore, W.S. and Shaw, T.J., 2008. Fluxes and Behavior of Radium Isotopes, Barium, and Uranium in Seven Southeastern US Rivers and Estuaries. *Marine Chemistry*, 108(3-4), pp. 236-254. doi:10.1016/j.marchem.2007.03.004
  36. Rutgers Van Der Loeff, M.M., Key, R.M., Scholten, J., Bauch, D. and Michel, A., 1995. <sup>228</sup>Ra as a Tracer for Shelf Water in the Arctic Ocean. *Deep Sea Research Part II: Topical Studies in Oceanography*, 42(6), pp. 1533-1553. doi:10.1016/0967-0645(95)00053-4
  37. Moore, W.S., Feely, H.W. and Li, Y.-H., 1980. Radium Isotopes in Sub-Arctic Waters. *Earth and Planetary Science Letters*, 49(2), pp. 329-340. doi:10.1016/0012-821x(80)90076-x
  38. Wang, G., Wang, S., Wang, Z. and Jing, W., 2018. Significance of Submarine Groundwater Discharge in Nutrient Budgets in Tropical Sanya Bay, China. *Sustainability*, 10(2), 380. doi:10.3390/su10020380
  39. Moore, W.S., Astwood, H. and Lindstrom, C., 1995. Radium Isotopes in Coastal Waters on the Amazon Shelf. *Geochimica et Cosmochimica Acta*, 59(20), pp. 4285-4298. doi:10.1016/0016-7037(95)00242-r
  40. Bituh, T., Petrinc, B., Marović, G., Senčar, J. and Gospodarić, I., 2008. <sup>226</sup>Ra and <sup>228</sup>Ra in Croatian Rivers. *Collegium Antropologicum*, 32(2), pp. 105-108.

41. Rutgers van der Loeff, M.M., Kühne, S., Wahsner, M., Höltzen, H., Frank, M., Ekwurzel, B., Mensch, M. and Rachold, V., 2003.  $^{228}\text{Ra}$  and  $^{226}\text{Ra}$  in the Kara and Laptev Seas. *Continental Shelf Research*, 23(1), pp. 113-124. doi:10.1016/s0278-4343(02)00169-3
42. Gurov, K.I., Ovsyany, E.I., Kotelyanets, E.A. and Kononov, S.K., 2015. Factors of Formation and Features of Physical and Chemical Characteristics of the Bottom Sediments in the Balaklava Bay (the Black Sea). *Physical Oceanography*, (4), pp. 46-52. doi:10.22449/1573-160X-2015-4-46-52
43. Kondrat'ev, S.I., Prusov, A.V. and Yurovskii, Yu.G., 2010. Observations of the Submarine Discharge of Underground Waters (South Coast of the Crimea). *Physical Oceanography*, 20(1), pp. 28-41. doi:10.1007/s11110-010-9065-3
44. Yurovsky, Yu.G., 2000. Evaluation of the Submarine Discharge of Karst Waters in the Region of Cape Aiya. *Physical Oceanography*, 10(3), pp. 283-286. doi:10.1007/BF02509225
45. Kondrat'ev, S.I., Shchetinin, Yu.T., Dolotov, N.N. and Androssovich, A.I., 1998. Hydrological and Chemical Characteristics of the Submarine Freshwater Source near Cape Aiya. *Physical Oceanography*, 9(3), pp. 217-224. doi:10.1007/BF02523232
46. Kondratev, S.I., Dolotov, V.V., Moiseev, Yu.G. and Shchetinin, Yu.T., 2000. Submarine Springs of Fresh Water in the Region from Cape Feolent to Cape Sarych. *Physical Oceanography*, 10(3), pp. 257-272. doi:10.1007/BF02509223
47. Aleskerova, A., Kubryakov, A., Stanichny, S., Medvedeva, A., Plotnikov, E., Mizyuk, A. and Verzhavskaia, L., 2021. Characteristics of Topographic Submesoscale Eddies off the Crimea Coast from High-Resolution Satellite Optical Measurements. *Ocean Dynamics*, 71(6-7), pp. 655-677. doi:10.1007/s10236-021-01458-9
48. Pasynkov, A.A. and Vakhrushev, B.A., 2017. The Submarine Water Sources in the South-East's Crimean Areas. *Scientific Notes of V. I. Vernadsky Crimean Federal University. Geography. Geology*, 3(2), pp. 250-263. doi:10.37279/2413-1717 (in Russian).
49. Kayukova, E.P. and Yurovsky, Y.G., 2016. Water Resources of the Crimea. *Geoecology. Engineering geology. Hydrogeology. Geocryology*, 1, pp. 25-32 (in Russian).
50. Aleskerova, A.A., Kubryakov, A.A., Goryachkin, Yu.N. and Stanichny, S.V., 2017. Propagation of Waters from the Kerch Strait in the Black Sea. *Physical Oceanography*, (6), pp. 47-57. doi:10.22449/1573-160X-2017-6-47-57
51. Drozhzhin, V.M., Nikolaev, D.S., Lazarev, K.F. and Grashchenko, S.M., 1973. Geochemical Balance of Radioactive Elements in the Black and Azov Seas. *Radiochemistry*, 15(3), pp. 415-421 (in Russian).
52. Key, R.M., Stallard, R.F., Moore, W.S. and Sarmiento, J.L., 1985. Distribution and Flux of  $^{226}\text{Ra}$  and  $^{228}\text{Ra}$  in the Amazon River Estuary. *Journal of Geophysical Research: Oceans*, 90(C4), pp. 6995-7004. doi:10.1029/JC090iC04p06995

*About the authors:*

**Ol'ga N. Kozlovskaya**, Junior Research Associate, Marine Hydrophysical Institute of RAS (2 Kapitanskaya Str., Sevastopol, 299011, Russian Federation), Junior Research Associate, Research Laboratory of Radioecology and Marine Radiochemistry, Sevastopol State University (33 Universitetskaya Str., Sevastopol, 299053, Russian Federation), **SPIN-code: 5386-4791**, o.n.kozlovskaya@gmail.com

**Dmitrii A. Kremenchutskii**, Senior Research Associate, Marine Hydrophysical Institute of RAS (2 Kapitanskaya Str., Sevastopol, 299011, Russian Federation), Ph.D. (Geogr.), **ORCID ID: 0000-0002-8747-6612**, **ResearchID: AAC-1673-2020**, d.kremenchutskii@mhi-ras.ru

**Yulia G. Shibetskaya**, Senior Engineer-Researcher, Marine Hydrophysical Institute of RAS (2 Kapitanskaya Str., Sevastopol, 299011, Russian Federation), **SPIN-code: 7765-8638**, iuliia.shibetskaia@gmail.com

**Viktoriya A. Razina**, Engineer, Marine Hydrophysical Institute of RAS (2 Kapitanskaya Str., Sevastopol, 299011, Russian Federation), **SPIN-code: 6754-8468**, razina.v@mail.ru

**Nikolay A. Bezhin**, Senior Research Associate, Marine Hydrophysical Institute of RAS (2 Kapitanskaya Str., Sevastopol, 299011, Russian Federation), Assistant Professor, Sevastopol State University (33 Universitetskaya Str., Sevastopol, 299053, Russian Federation), Ph.D. (Tech.), **ORCID ID: 0000-0002-1670-4251**, nickbezhin@yandex.ru

*Contribution of the co-authors:*

**Ol'ga N. Kozlovskaya** – conceptualization, formal analysis, investigation, data curation, writing of the original draft, review and editing

**Dmitrii A. Kremenchutskii** – conceptualization, formal analysis, investigation, visualization, writing of the original draft, review and editing

**Yulia G. Shibetskaya** – data curation, investigation

**Viktoriya A. Razina** – data curation, investigation

**Nikolay A. Bezhin** – conceptualization, formal analysis, investigation, data curation, review and editing of the original draft

*The authors have read and approved the final manuscript*

*The authors declare that they have no conflict of interest*